NASA TECHNICAL NOTE

NASA TN D-3418

NASA TN D-3418

AN EXPLORATORY INVESTIGATION OF FACTORS AFFECTING THE HANDLING QUALITIES OF A RUDIMENTARY HINGELESS ROTOR HELICOPTER

by Robert J. Huston

Langley Research Center
Langley Station, Hampton, Va.

NATIONAL AERONAUTICS AND SPACE ADMINISTRATION • WASHINGTON, D. C. • MAY 1966

NASA TN D-3418

AN EXPLORATORY INVESTIGATION OF FACTORS AFFECTING THE HANDLING QUALITIES OF A RUDIMENTARY HINGELESS ROTOR HELICOPTER

By Robert J. Huston

Langley Research Center
Langley Station, Hampton, Va.

NATIONAL AERONAUTICS AND SPACE ADMINISTRATION

For sale by the Clearinghouse for Federal Scientific and Technical Information
Springfield, Virginia 22151 – Price $2.00

AN EXPLORATORY INVESTIGATION OF FACTORS AFFECTING THE HANDLING QUALITIES OF A RUDIMENTARY HINGELESS ROTOR HELICOPTER

By Robert J. Huston
Langley Research Center

SUMMARY

A flight investigation was conducted to study the handling qualities of a rudimentary hingeless rotor helicopter. The results indicate that the control characteristics were generally good with positive and precise pitch control. The roll control response was generally good but pilots objected to a pitch-due-to-roll angular-velocity coupling. The coupling was shown to be predictable and methods are available to minimize the coupling. The hingeless rotor helicopter was found to have positive maneuver stability and good damping of moderate gust disturbances up to the maximum speed obtainable.

INTRODUCTION

The problem areas and advantages offered by the hingeless rotor helicopter configuration are being investigated by the NASA Langley Research Center. One area of general interest is the potential improvement in flying qualities made possible by increased control moment per degree of cyclic blade pitch and by a substantial increase in angular-velocity damping. An exploratory flight-test program utilizing a three-blade hingeless rotor installed on an OH-13 helicopter was made to study the potential improvement in handling qualities and some of the problems associated with the system.

The aircraft utilized in this investigation is not an optimum design for a hingeless rotor helicopter inasmuch as it was assembled almost entirely from existing articulated rotor parts. Some deficiencies in the overall handling qualities of the helicopter would be expected because of the rudimentary hardware used. Some limited experimental results obtained with this helicopter and an identical helicopter have been published in references 1, 2, and 3.

The present report covers some measurements of control response characteristics in hover and forward flight, comparison of hovering response characteristics with simple theoretical calculations, general characteristics, and pilot comments. The control

response characteristics are studied in detail in order to explain the cross-coupling phenomenon which occurs during maneuvers with the hingeless rotor.

Comments were obtained from several pilots, with experience ranging from 12 to 20 years of helicopter handling qualities evaluation.

This report includes an appendix by Robert J. Huston and William J. Snyder which presents an analysis and discussion of the angular-velocity response of a hingeless rotor helicopter.

SYMBOLS

Measurements for this investigation were taken in the U.S. Customary System of Units. Equivalent values are indicated herein in the International System (SI) in the interest of promoting the use of this system in future NASA reports.

A_0 mean blade pitch angle at three-quarter radii, deg

A_1 coefficient of $-\cos\psi$ in expression for θ, positive for nose up at $\psi = 180^o$, deg

a slope of curve of lift coefficient against angle of attack, per radian

a' angle between control axis and rotor resultant force vector in longitudinal plane, radians

B_1 coefficient of $-\sin\psi$ in expression for θ, positive for nose up at $\psi = 270^o$, deg

b' angle between control axis and rotor resultant force vector in lateral plane, radians

C_T rotor thrust coefficient, $\frac{T}{\pi R^2 \rho(\Omega R)^2}$

c blade chord, ft (m)

H gyroscopic moment proportional to angular velocity, positive pitching moment with positive rolling velocity for clockwise rotating rotor, lbf-ft/radian/sec (N-m/radian/sec)

h vertical distance between aircraft center of gravity and rotor hub, ft (m)

I_V blade mass moment of inertia about virtual hinge, slug-ft^2 (kg-m^2)

I_X aircraft mass moment of inertia about body longitudinal axis, slug-ft^2 (kg-m^2) (790 slug-ft^2 (1071 kg-m^2) in calculations)

I_Y aircraft mass moment of inertia about body lateral axis, slug-ft^2 (kg-m^2) (1700 slug-ft^2 (2305 kg-m^2) in calculations)

M_A longitudinal aircraft moment, lbf-ft (N-m)

M_B lateral aircraft moment, lbf-ft (N-m)

M_p damping moment proportional to and opposing rolling velocity, lbf-ft/radian/sec (N-m/radian/sec)

M_q damping moment proportional to and opposing pitching velocity, lbf-ft/radian/sec (N-m/radian/sec)

$M_{H,A}$ longitudinal hub moment for $\epsilon = 0$, positive for nose up moment, lbf-ft (N-m)

$M_{H,B}$ lateral hub moment for $\epsilon = 0$, positive for roll right moment, lbf-ft (N-m)

$M_{x_{\delta_x}}$ rate of change of lateral hub moment with respect to lateral stick displacement, lbf-ft/in. (N-m/cm)

$M_{x_{\delta_y}}$ rate of change of lateral hub moment with respect to longitudinal stick displacement, lbf-ft/in. (N-m/cm)

$M_{y_{\delta_x}}$ rate of change of longitudinal hub moment with respect to lateral stick displacement, lbf-ft/in. (N-m/cm)

$M_{y_{\delta_y}}$ rate of change of longitudinal hub moment with respect to longitudinal stick displacement, lbf-ft/in. (N-m/cm)

p rolling velocity, positive when rolling to right, radians/sec

$\dot{p}$ rolling acceleration, radians/sec/sec

q pitching velocity, positive when pitching nose up, radians/sec

$\dot{q}$	pitching acceleration, radians/sec/sec
R	rotor radius, ft (m)
T	thrust, lbf (N)
t	time, sec
V	airspeed, knots
γ	mass constant of rotor blade (blade Lock number), $\frac{\rho a c R^4}{I_V}$.
Δ	increment
δ_x	lateral stick deflection, positive to right, in. (cm)
δ_y	longitudinal stick deflection, positive aft, in. (cm)
ϵ	control retardation angle, deg
θ	blade pitch angle at any azimuth position ψ, deg
ρ	mass density of air, slugs/cu ft (kg/m^3)
σ	rotor solidity, ratio of total blade area to rotor disk area
ψ	blade azimuth angle measured from downwind position in direction of rotation, deg
Ω	rotor angular velocity, radians/sec
ω_{1NR}	cantilever first mode flapwise natural frequency of nonrotating blade, radians/sec

Subscripts:

A_1	due to A_1
B_1	due to B_1
p	due to p

q	due to q
∞	$t = \infty$
max	maximum
trim	trim conditions

TEST AIRCRAFT AND TEST PROCEDURE

The test aircraft, shown in figure 1, was assembled by replacing the teetering rotor on a standard Army OH-13G helicopter with a nonarticulated hub, and three slightly shortened OH-13H helicopter metal blades. In addition, the stabilizer bar and horizontal tail of the standard helicopter were removed.

(a) General view of aircraft. L-62-6643

Figure 1.- Hingeless rotor helicopter.

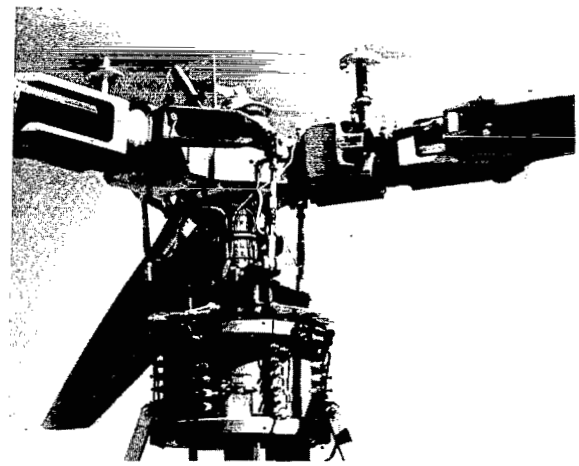

(b) Rotor hub and slipring assembly. L-62-6644

Figure 1.- Concluded.

The physical characteristics of the test aircraft, as modified, are listed in the following table:

Main rotor:	
Diameter	31.66 ft (9.65 m)
Blade chord (constant root to tip)	11 in. (27.94 cm)
Solidity, σ	0.055
Blade airfoil section	NACA 0015
Nominal tip speed	588 ft/sec (179.2 m/sec)
Blade twist, root to tip, deg	-7
Blade Lock number	3.85
Aircraft:	
Nominal take-off weight	2260 lbf (10 052 N)
Longitudinal center of gravity, forward of rotor mast	0.15 in. (0.381 cm)
Vertical center of gravity, below rotor hub center	5 ft (1.52 m)
Roll moment of inertia	790 slug-ft^2 (1071 kg-m^2)
Pitch moment of inertia	1700 slug-ft^2 (2305 kg-m^2)

The travel of the pilot's grip on the control stick was 11.5 inches (29.21 cm) along a circular arc for both longitudinal and lateral axes. Control springs provided a spring gradient of 1/2 pound per inch (89 N/m) of travel of the pilot's grip in both axes. Both cyclic controls had light moving friction (less than 1/2 pound (2.224 N) at the pilot's grip), but movement of the lateral control required approximately an additional 3/4 pound (3.34 N) to break the valve friction in the boost system. The cyclic control system was

that of a standard OH-13G helicopter except for a modification that provided mixing of the stick control inputs to the blade. The resulting cyclic feathering due to control mixing occurred as given in the following equations:

$$\Delta A_1 = 0.926\Delta\delta_x + 0.538\Delta\delta_y \quad (1)$$

$$\Delta B_1 = 0.482\Delta\delta_x - 1.034\Delta\delta_y \quad (2)$$

The travel of the collective stick grip was 11 inches (27.94 cm) along a circular arc and resulted in a collective pitch change of 11°. The directional control system was standard for an OH-13 helicopter.

The rotor mast and transmission were standard OH-13G installations. The mast and transmission assembly sit in dual trunnions with longitudinal and lateral restraints provided by two rubber cushioned lower mast mounts installed 31.5 inches (0.8 m) below the trunnions. The center of the rotor hub is approximately 50 inches (1.27 m) above the trunnions. After initial flights with the standard mounts installed, both the longitudinal and lateral mounts were replaced with mounts having higher spring constants in order to change the effective pylon stiffness. The measured characteristics of the two sets of mounts are listed in the following table:

Lower mast mount	Limit longitudinal travel				Limit lateral travel				Spring constant	
	Forward		Aft		Right		Left			
	in.	cm	in.	cm	in.	cm	in.	cm	lb/in.	N/m
Stiff	0.50	1.27	0.75	1.90	0.75	1.90	0.50	1.27	1205	211 030
Standard	0.30	0.76	0.13	0.33	0.77	1.96	0.57	1.45	618	108 230

The aircraft was limited in performance; throughout the test program the helicopter was unable to hover out of ground effect because of the increased weight of test instrumentation and the bulky overweight components used to make up the test vehicle. In addition, a power required increase was obtained by adding a third blade and reducing the rotor radius.

The task used to evaluate the handling qualities of the aircraft included longitudinal and lateral control steps, control pulses, and control reversals throughout the speed range. Additional maneuvers were performed to identify any handling qualities problem area not apparent in the previous test maneuvers. These maneuvers were vertical autorotation, autorotation at airspeeds up to 70 knots, partial power descents in the vortex ring state, maximum power climb through the speed range, and steep turns in level flight and autorotation.

Some limited data were obtained after conclusion of the hingeless rotor flight tests with the teetering rotor installed on the test vehicle. The instrumentation used to measure the handling qualities characteristics remained installed during the rotor change and were used throughout both portions of the test program. The data obtained with the teetering rotor helicopter include the effects of the standard horizontal tail and stabilizer bar that are normally installed.

RESULTS AND DISCUSSION

Hovering Control Response

The handling qualities investigation with the hingeless rotor helicopter was directed toward determining the extent to which the increased angular-velocity damping and control sensitivity contribute to an improvement in overall handling qualities. To a very great extent the much tighter response of the hingeless rotor helicopter was reflected in the pilots' willingness to maneuver under marginal conditions. In spite of marginal hovering performance all pilots found that the aircraft could be maneuvered adequately near zero airspeed while very close to the ground.

One adverse factor noted by the pilots, which became the subject of analytical examination, was a strong cross-coupling of the angular-velocity response between the pitch and roll axes. Inasmuch as the mechanism producing the angular-velocity cross-coupling and the tight response are directly related, a discussion of the theoretical first-order response is presented prior to presentation of the measured aircraft response. The sources of the control and damping moments have been previously covered in references 3 and 4.

Response characteristics of a hingeless rotor.- The increased control and damping moment capability of the hingeless rotor is obtained by transmittal of once-per-revolution cyclic blade moments through the cantilever action of the blades to the rotor hub and to the aircraft.

The first result of the cantilever action of the blades, from the control design standpoint, is that the desired control moment is obtained more closely in phase with the applied cyclic blade pitch than with a simple flapping rotor. (See shaded area in fig. 2.) The reduced phase lag occurs because the cantilevered blade is being forced at a frequency slightly below the first bending mode natural frequency of the blade instead of at resonance, which is the case for a simple flapping rotor. The reduced phase lag of the hingeless rotor requires that the lead angle of the cyclic blade pitch be reduced (or retarded) from the 90° lead of the simple flapping rotor in order to prevent direct control coupling. The initial rotor tip-path-plane tilt (and hub moment), in response to a control stick movement, is therefore in the direction of the stick movement when the correct

control retardation is used. In addition, the correct control retardation allows the changes in trim stick position with airspeed to correspond to the required cyclic feathering of the rotor. That is, the required longitudinal and lateral cyclic pitch for a trim condition is reflected by corresponding longitudinal and lateral stick travel.

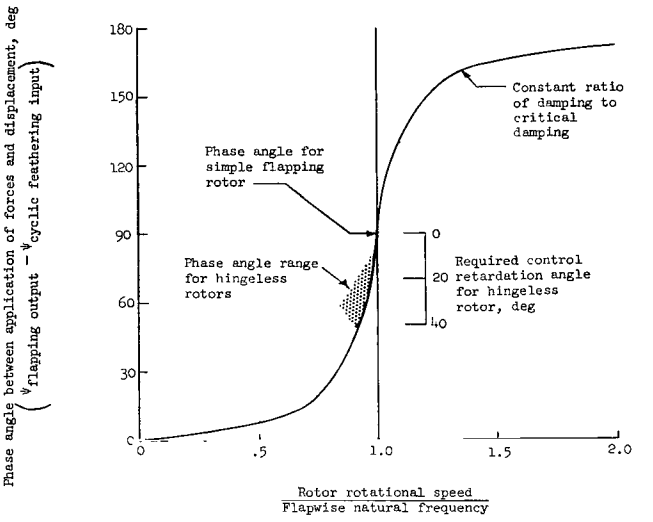

Figure 2.- Variation of response phase angle with flapwise natural frequency.

The second result of the cantilever action of the blades is a gyroscopic coupling of the angular-velocity damping; the amount of coupling is a function of the cantilever mode frequency and damping. The damping coupling results in a combined pitch and roll response during transients from trim condition to steady-state pitch and/or roll rates and in the direction of the steady-state angular velocities being different from the initial response direction (or initial direction of tip-path-plane tilt). Therefore, a pure pitch or roll maneuver would require a cross controlling of longitudinal and lateral stick position; the amount varies with time, even with the correct control retardation installed. For a specific blade design the damping coupling, when present, can only be eliminated by a control feedback device such as that suggested in reference 4; however, the direct coupling can be eliminated by building in the correct control retardation.

The total action of the direct coupling and damping coupling can be best understood by an illustration. The calculated first-order response to a longitudinal and lateral 1-inch (2.54-cm) step control input are given in figures 3(a) and 3(b), respectively. The calculated time histories are based on the results presented in reference 3 and appendixes A and B and are for hovering maneuvers without the effects of translational velocity (i.e., there is no dihedral effect or speed stability). This result has been cross plotted in figure 4 with the pitching angular velocity plotted against rolling angular velocity. The arrows and symbols around the edge of figure 4 indicate the direction (combination of pitching velocity and rolling velocity) of the aircraft response and can be identified as an aircraft rotation about an axis that is perpendicular to some stated azimuth position ψ on the rotor disk. The end point of the calculated curves in figure 4 represents the steady-state pitching and rolling angular velocities shown in figure 3.

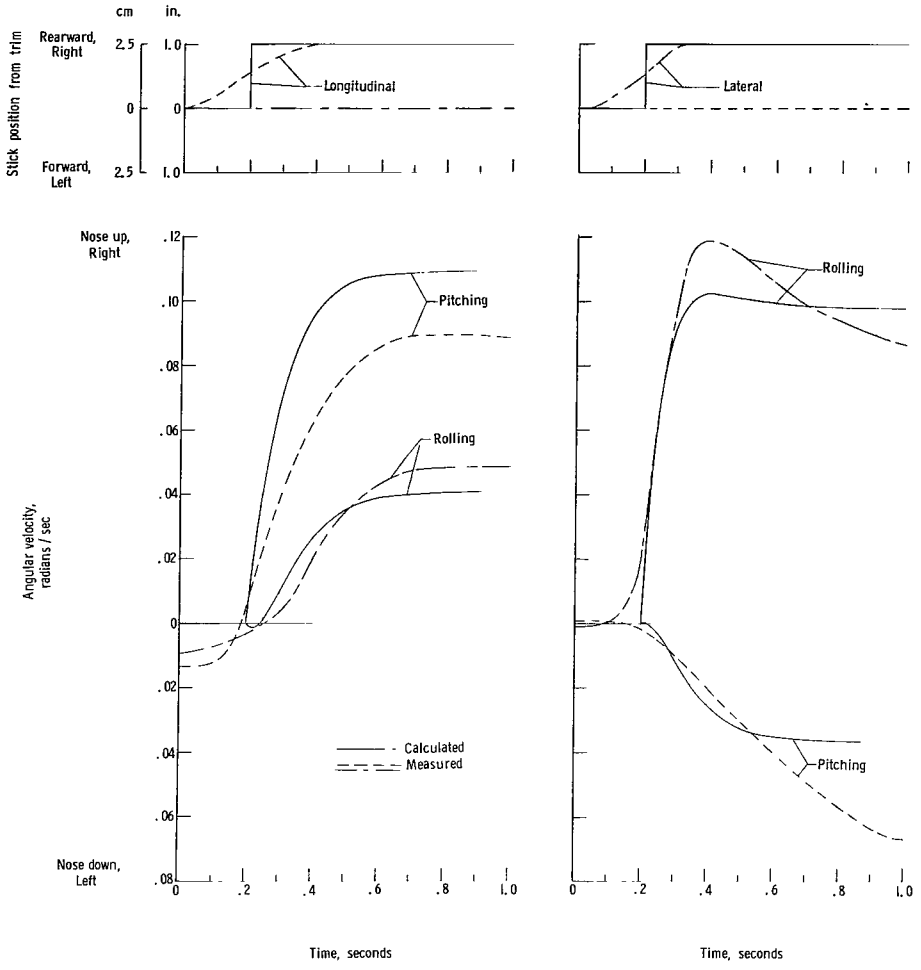

(a) Longitudinal step input.

(b) Lateral step input.

Figure 3.- Computed time histories of angular velocities resulting from step input with a comparison of the measured response of the hingeless rotor helicopter with stiff mount installation. Hovering.

Calculated response.- Without control retardation, a pure back stick control input results in maximum nose-up blade pitch occurring at the $\psi = 90^{o}$ blade position (direction ①, fig. 4). The resulting response, for the test aircraft without control retardation, is an initial tilt of the tip-path plane which theoretically occurs in the direction of the $\psi = 148^{o}$ position (direction ②) or approximately 58^{o} after the maximum cyclic feathering at $\psi = 90^{o}$. Because the hub moment is applied to unequal body inertias ($I_Y > I_X$), the initial angular acceleration of the aircraft occurs in the direction of the $\psi = 132^{o}$ position (direction ③).

With the 27.5^{o} of control retardation actually installed in the test aircraft, a pure nose-up longitudinal step control stick input results in maximum cyclic feathering

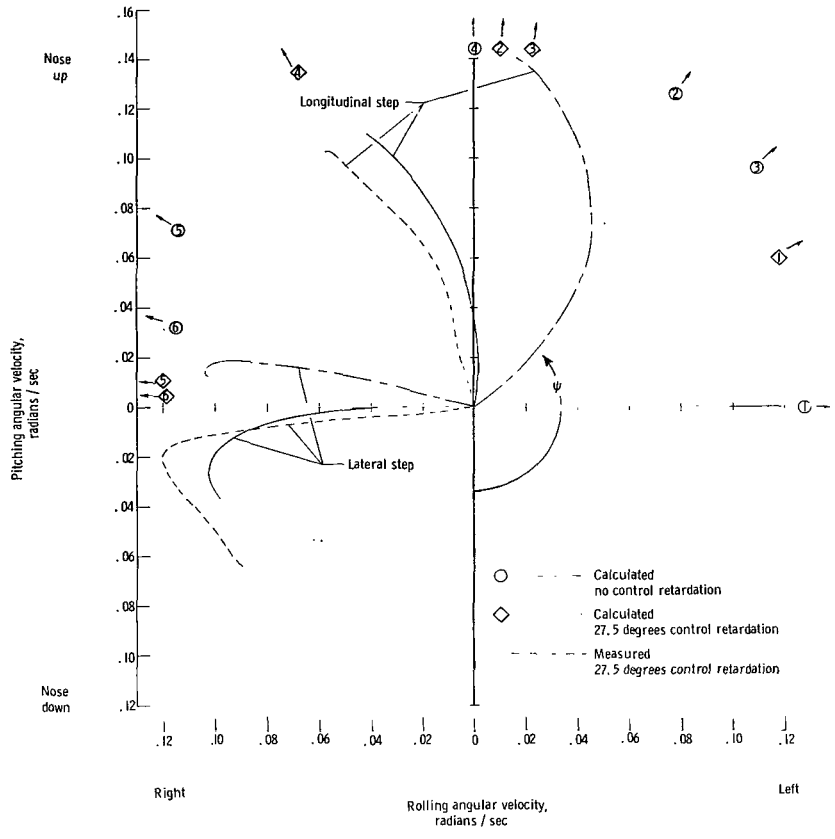

Figure 4.- Calculated angular-velocity response to 1-inch (2.54-cm) longitudinal and lateral step with a comparison with measured hingeless rotor response. Direction of theoretical response to longitudinal step illustrated as ①, ◇1 blade cyclic feathering input; ②, ◇2 initial tip-path-plane tilt; and ③, ◇3 initial aircraft angular acceleration. Direction of theoretical response to lateral step illustrated as ④, ◇4 blade cyclic feathering input; ⑤, ◇5 initial tip-path-plane tilt; and ⑥, ◇6 initial aircraft angular acceleration.

occurring at $\psi = 117.5^{o}$ (direction ◇1, fig. 4) instead of at $\psi = 90^{o}$. The initial tilt of the tip-path plane theoretically occurs in the direction of the $\psi = 176^{o}$ position (direction ◇2), or still 58^{o} after maximum cyclic feathering, and the initial angular acceleration of the aircraft occurs in the direction of the $\psi = 171^{o}$ position (direction ◇3).

The damping cross-coupling, for the case of no control retardation, will cause a resultant steady-state angular velocity in the direction of $\psi = 173^{o}$ position as illustrated by the end of the calculated curve in figure 4. With no control retardation, a noticeable reversal of roll acceleration occurs, as evidenced by the reduction in roll velocity. With the 27.5^{o} control retardation actually installed in the test aircraft, the steady-state angular velocity theoretically occurs in the direction of the $\psi = 200.5^{o}$ position, or 27.5^{o} later than without the control retardation.

A similar theoretical response to a pure right roll step is also illustrated in figure 4 for both no control retardation and 27.5^{o} of control retardation.

Measured response.- For comparison with the theoretical response curves for the 27.5° control retardation, the measured change in pitch and roll angular velocities for 1-inch (2.54-cm) longitudinal and 1-inch (2.54-cm) lateral "step" inputs is also plotted in figures 3 and 4. These results show reasonable agreement with the predicted response. In order to allow for the fact that the actual "step" was a ramp input taking 0.3 to 0.4 second to complete, the theoretical step is arbitrarily commenced at t = 0.2 second in figure 3 to better distinguish the slope differences between the theoretical and actual response. One characteristic apparent in both the theoretical (27.5° control retardation) and measured response curves is the overshoot in the roll response to a lateral step.

The measured response curves presented in figures 3 and 4 are for the stiff mast mount installation. A comparison of the theoretical response with the measured response with the standard mounts installed is given in figure 5. The previously discussed

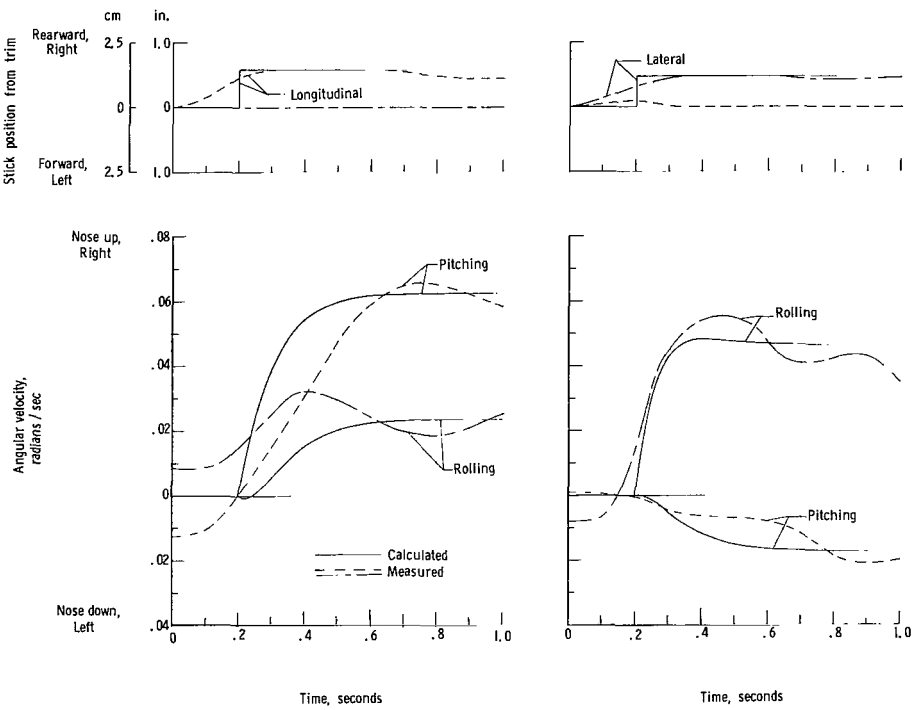

(a) Longitudinal step input.

(b) Lateral step input.

Figure 5.- Computed time histories of angular velocities resulting from step input with a comparison of the measured response of the hingeless rotor helicopter with standard mount installation. Hovering.

tendency to overshoot the final steady-state angular velocity for roll inputs was also found for the standard mount installation along with a general oscillation about both axes.

Pilot evaluation of control response.- In the opinion of the pilots, the overall hovering control characteristics (control sensitivity and angular-velocity damping) were considered good. Pitch control was positive, precise, and not overly sensitive.

The angular-velocity response to a roll control input appeared, to the pilot, to be oscillatory. The final rolling velocity reached was lower than expected, considering the high initial acceleration and the rolling velocity peak initially obtained. The oscillatory character and the overshoot tendency of the roll response was considered objectionable to the pilots. The valve friction in the lateral boost system did produce a tendency for lateral overcontrolling to a moderate degree but it was not considered dangerous by the pilots.

The gyroscopic coupling was considered undesirable. The pitching angular velocity produced by roll inputs was considered large and objectionable for any but gentle maneuvers, although it was considered controllable. Accurate control of the pitch attitude during a rolling maneuver, however, was considered difficult by the pilots because of the large magnitude of the coupling. The roll angular velocity produced by a pitch input, for the test aircraft, was considered by the pilots to be small and not of any consequence.

Discussion of pilot comments.- The overshoot tendency of the roll response of the test aircraft, which is indirectly due to the gyroscopic coupling of the hingeless rotor, was amplified by overcontrolling due to boost-valve friction and an oscillation in the roll response. The roll oscillation, which was found present with the standard mast mount installation, was substantially reduced for small control movements when the stiff mounts were installed. (See figs. 3 and 5.) With large lateral control movements, however, the lateral oscillation is still excited about the mean rolling velocity (fig. 6). The nonlinear character of the oscillation appears to be due to extending the lower mast mounts to their limit travel. In addition, cyclic control washout due to mast bending, as noted in reference 1, will provide an oscillatory control input at the natural frequency of the mount installation. Each of these terms (gyroscopic coupling, pylon frequency, nonlinearity, and control washout) contribute to the oscillatory character and overshot tendency at the roll response which was considered objectionable to the pilots. The significance of each of these terms, for future designs, will have to be individually assessed.

The gyroscopic coupling was found to be undesirable because of the high coupled pitching acceleration resulting from a roll control input. A comparison of the time histories for the hingeless rotor (figs. 7 and 8) and the teetering rotor helicopter (fig. 9) shows that the ratio of the steady-state angular-velocity coupling p/q is nearly the same for the two aircraft. The time constant of the coupled angular-velocity response of the hingeless rotor, however, is shorter than that of the teetering rotor response, and the

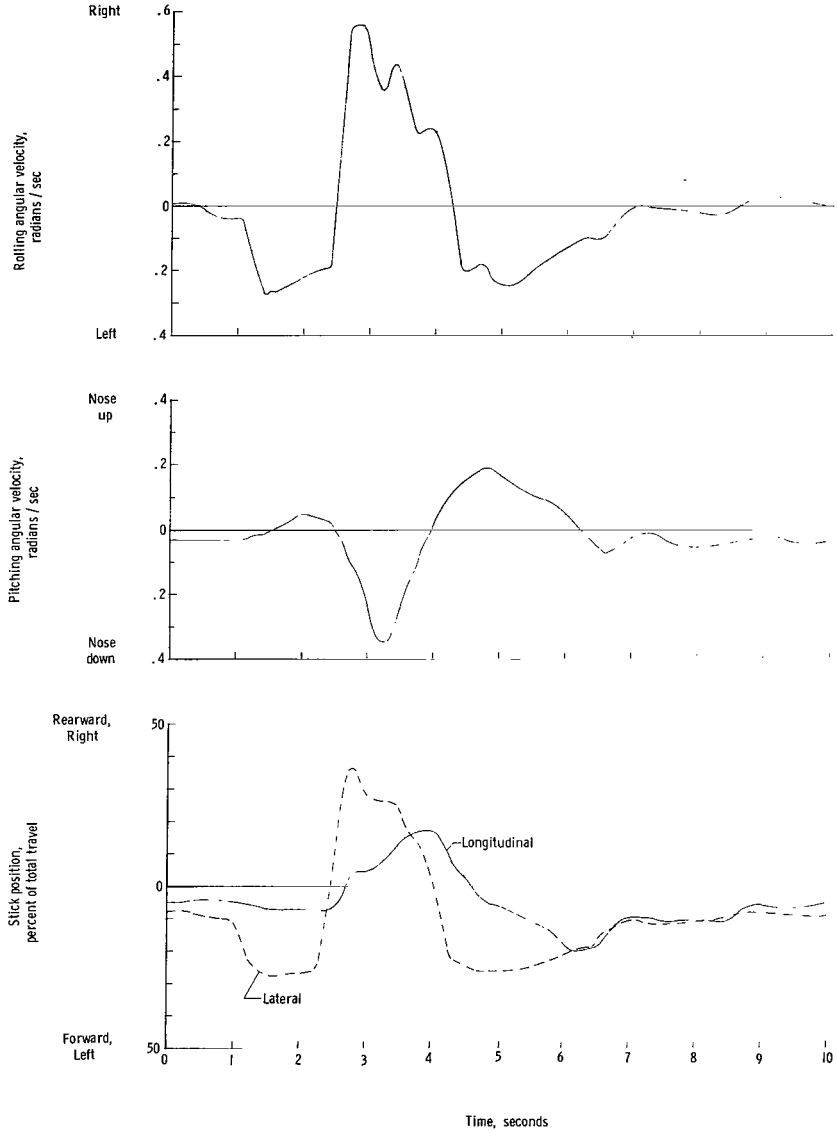

Figure 6.- Time history of angular velocities resulting from rapid roll reversal maneuver where pilot attempts to control pitch cross-coupling response. Hovering. Hingeless rotor helicopter with stiff mount installation.

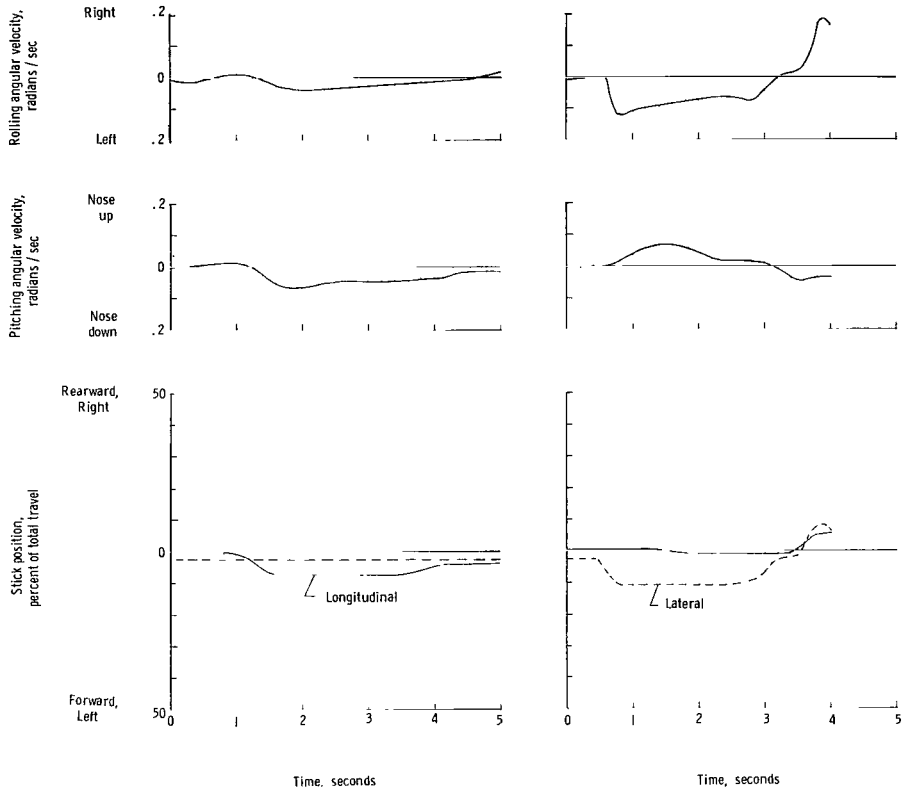

(a) Longitudinal step input.

(b) Lateral step input.

Figure 7.- Time histories of angular velocities resulting from step control input. Hovering. Hingeless rotor helicopter with stiff mount installation.

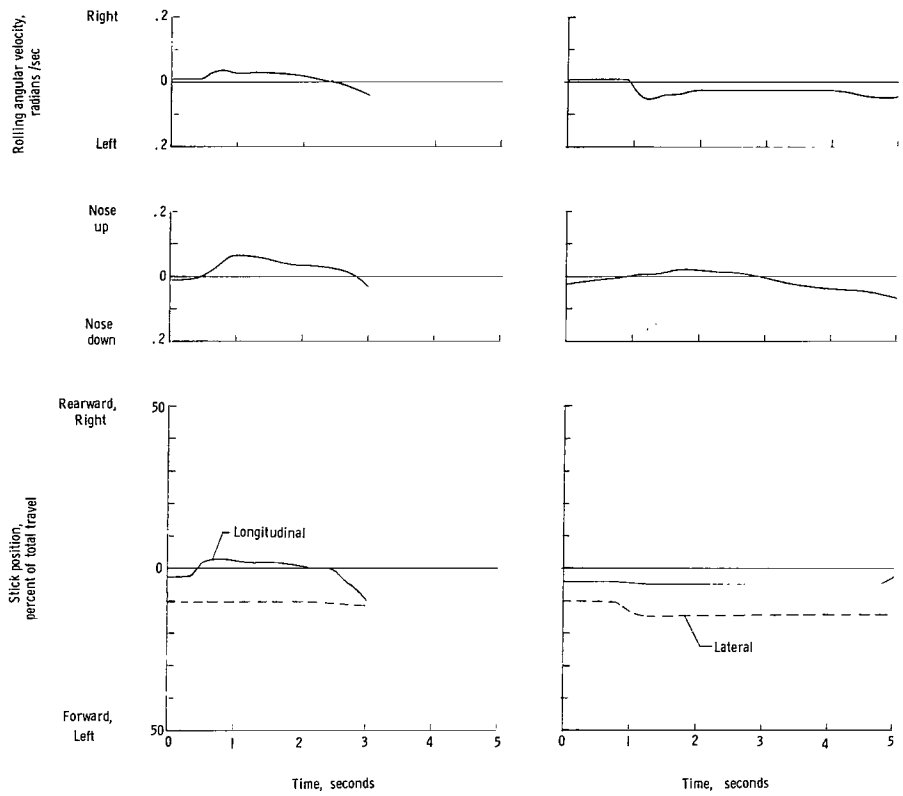

(a) Longitudinal step input.

(b) Lateral step input.

Figure 8.- Time histories of angular velocities resulting from step control input. Hovering. Hingeless rotor helicopter with standard mount installation.

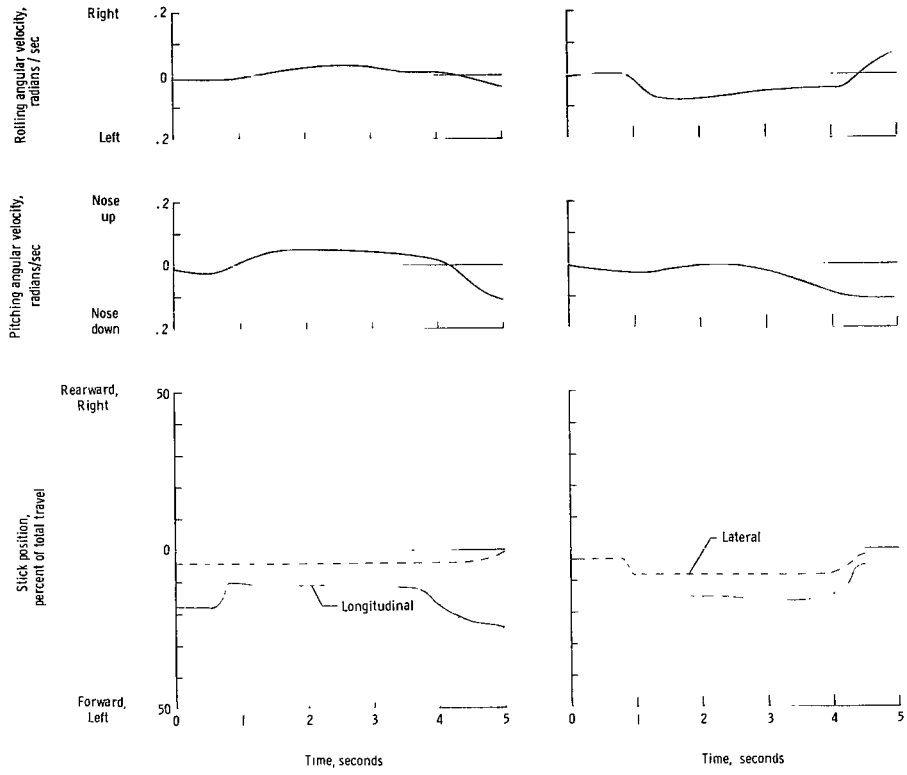

(a) Longitudinal step input.

(b) Lateral step input.

Figure 9.- Time histories of angular velocities resulting from step control input. Hovering. Teetering rotor.

angular acceleration of the coupled velocity is higher. It appears that this shorter time constant is the basis for the undesirable evaluation of the hingeless rotor coupling by the pilots. The smaller time constant and high angular acceleration of the coupled velocity are particularly apparent in figure 6 where, during a rapid roll reversal, the pitch input by the pilot is insufficient to arrest the coupled pitching velocity and the pilot tends to overcorrect and get out of phase. It was noted in reference 5 that the pilot, in an investigation of gyroscopic coupling, rates the ratio of pitch acceleration to roll velocity $\dot{q}/p$ (the maximum value of $\dot{q}$ obtained divided by the steady-state value of p) rather than the magnitude of the cross-coupling moment H. In the case of the hingeless rotor the pilot is also rating $\dot{q}/p$, although it should be noted that the response of the test aircraft includes the effect of an insufficient amount of control retardation and therefore there is a direct coupled response as well as a gyroscopic coupled response. The direct coupling is apparent in figures 3 and 4 as the initial direction of the calculated coupled angular velocities.

The pilots' acceptance of the pitch coupling occurring with a roll input is in agreement with the results of reference 5. The range of coupling for the investigation of reference 5 is given in the following table, along with the value of coupling where, in the pilots' opinion, the controllability of the coupling became marginal. The computed cross-coupling of the hingeless rotor is presented for comparison in the following table:

	Pitch due to roll		Roll due to pitch	
	H/I_Y	H/M_q	H/I_X	H/M_p
Upper limit of parameters investigated in reference 5	1.40	3.93	1.05	0.841
Value of parameters where pilot rated controllability marginal for steep turns and roll reversals in reference 5	0.22	0.617	Marginal limit not reached	
Computed parameters for hingeless rotor helicopter	3.53	0.46	7.60	0.46

The ratio of cross-coupled damping moment to inertia H/I_X was used in reference 5 as the primary variable under consideration. However, it was pointed out that the direct damping in the axis of the coupled response will alter the pilot's acceptability of the coupled response. A comparison of the computed ratio of gyroscopic moment to damping moment $\left(H/M_p \text{ or } H/M_q\right)$ of the test aircraft with the results of reference 5 indicates that these ratios are below the range investigated in reference 5. (See preceding table.)

The ratio of gyroscopic moment to roll damping moment H/M_p of the test aircraft is substantially below that investigated in reference 5 and caused no difficulty for any maneuver task. The ratio of gyroscopic moment to pitch damping moment H/M_q of the test aircraft is slightly below the value found to result in marginal control. (See preceding table.) It appears that the undesirability of this amount of coupling on the hingeless rotor is due to the increased initial acceleration of the coupled pitch response of the hingeless rotor with perhaps some additional deterioration in handling qualities because of the direct cross-coupling.

The pilots noted that, in rolling maneuvers, the final steady rolling velocity reached was always lower than expected. This result is partially due to the overshoot related to the cross-coupled damping; however, the dihedral effect is a more significant influence. The dihedral effect (and speed stability), in terms of moment-to-body-inertia ratio, is increased over that of an articulated rotor by the same ratio as the control moment per degree of cyclic blade angle. The high dihedral effect results in a reduction of rolling angular velocity (see figs. 3 and 7) within the first second after a roll control input. While not separately discernible to the pilot, the dihedral effect also results in an increase in the coupled pitching velocity due to the direct coupling. (That is, the dihedral effect acts as a lateral cyclic pitch change where the resultant hub moment occurs approximately 58° in azimuth position after the effective cyclic pitch change.) Therefore, a left rolling moment induced by the dihedral effect will be coupled with a nose-down moment. (See fig. 4 curve with no control retardation.) This action is also present in a pitch maneuver, but the speed stability, in terms of moment-to-body-inertia ratio, is less than half of the dihedral effect because the body pitching moment of inertia is greater than twice the body rolling moment of inertia. The direct coupling associated with speed stability and dihedral effect can only be eliminated by some type of control feedback device.

Forward Flight Control Response

The response of the hingeless rotor test aircraft to longitudinal and lateral step control inputs at approximately 65 knots is presented in figure 10 for the stiff pylon mounts and in figure 11 for the standard pylon mounts. Similar response characteristics for the two-bladed teetering-rotor H-13 are presented in figure 12 for comparison. For both levels of mast mount stiffness the time history of the normal acceleration to a pull-and-hold maneuver appears concave downward within approximately 2 seconds. A short-period oscillation appears to be slightly more pronounced for the stiff pylon installation than for the standard mounts with the pull-and-hold maneuver. The response to a lateral step input with both mount installations has the characteristic initial roll overshoot which was found objectionable to the pilots for hovering. The overshoot characteristic was also

considered objectionable by the pilots in forward flight. The oscillatory roll response, as in hovering, again appears more prominent for the standard mounts than for the stiff mounts.

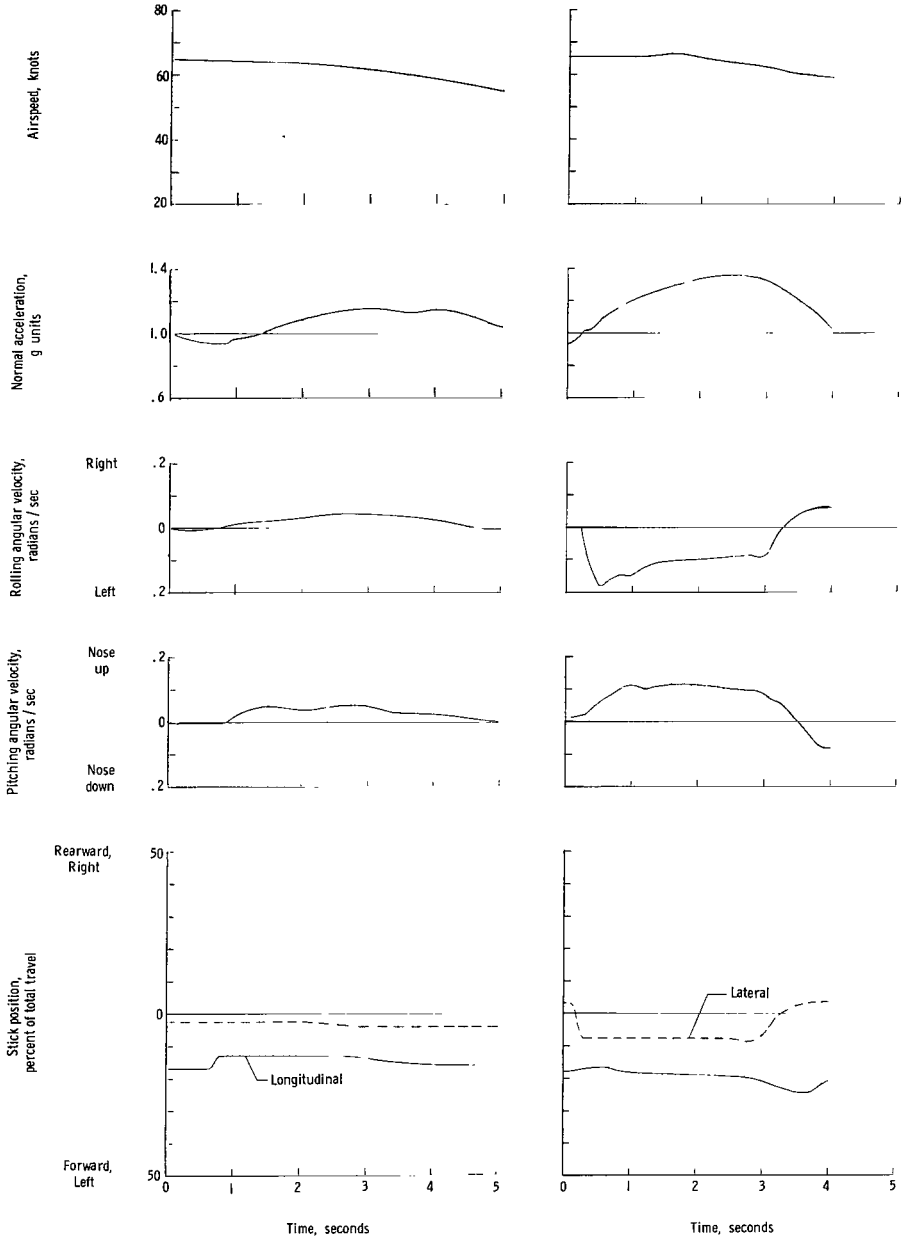

(a) Longitudinal step input.

(b) Lateral step input.

Figure 10.- Time histories of normal acceleration and angular velocities resulting from step control inputs in forward flight. Hingeless rotor helicopter with stiff mount installation.

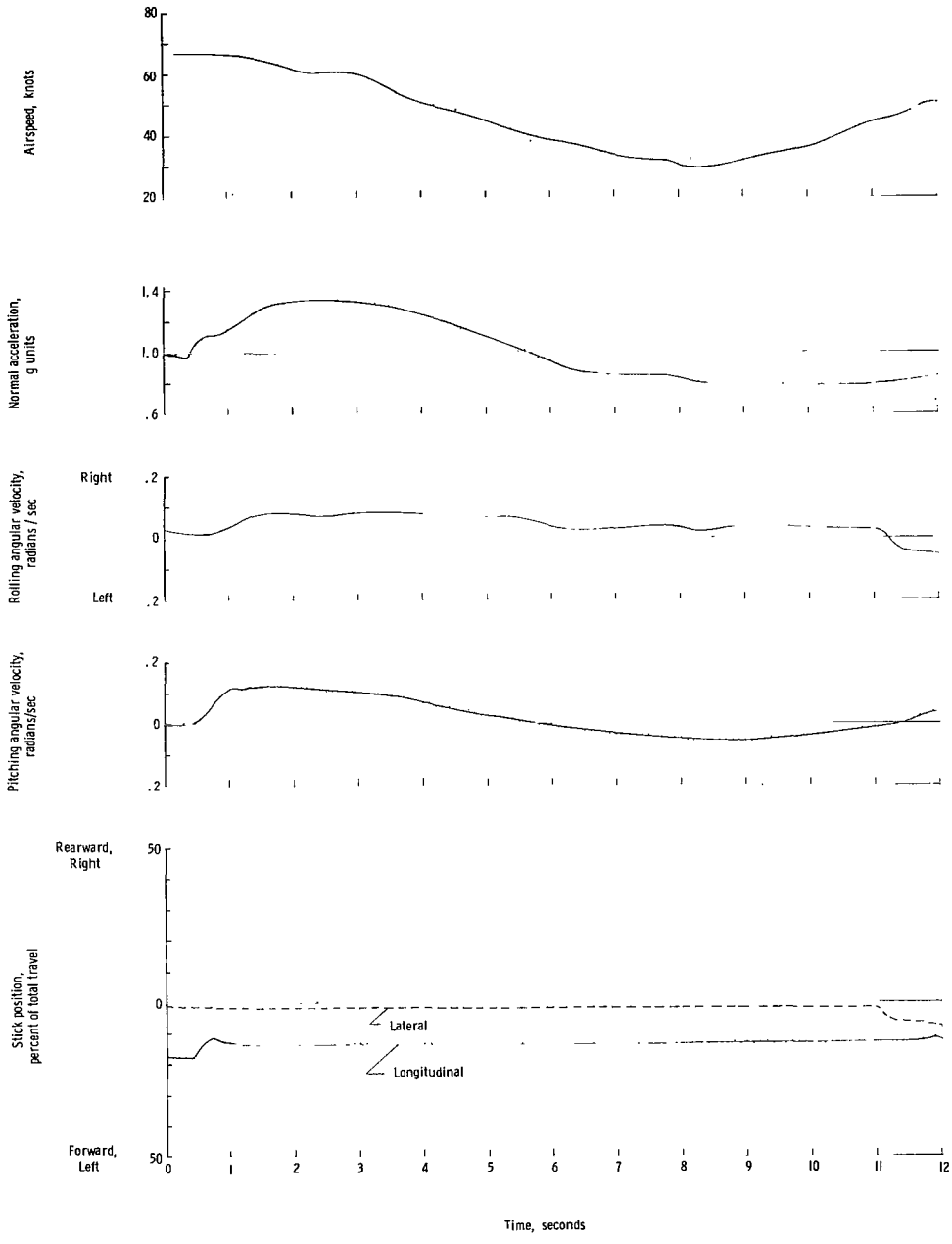

(a) Longitudinal step input.

Figure 11.- Time histories of normal acceleration and angular velocities resulting from step control input in forward flight. Hingeless rotor helicopter with standard mount installation.

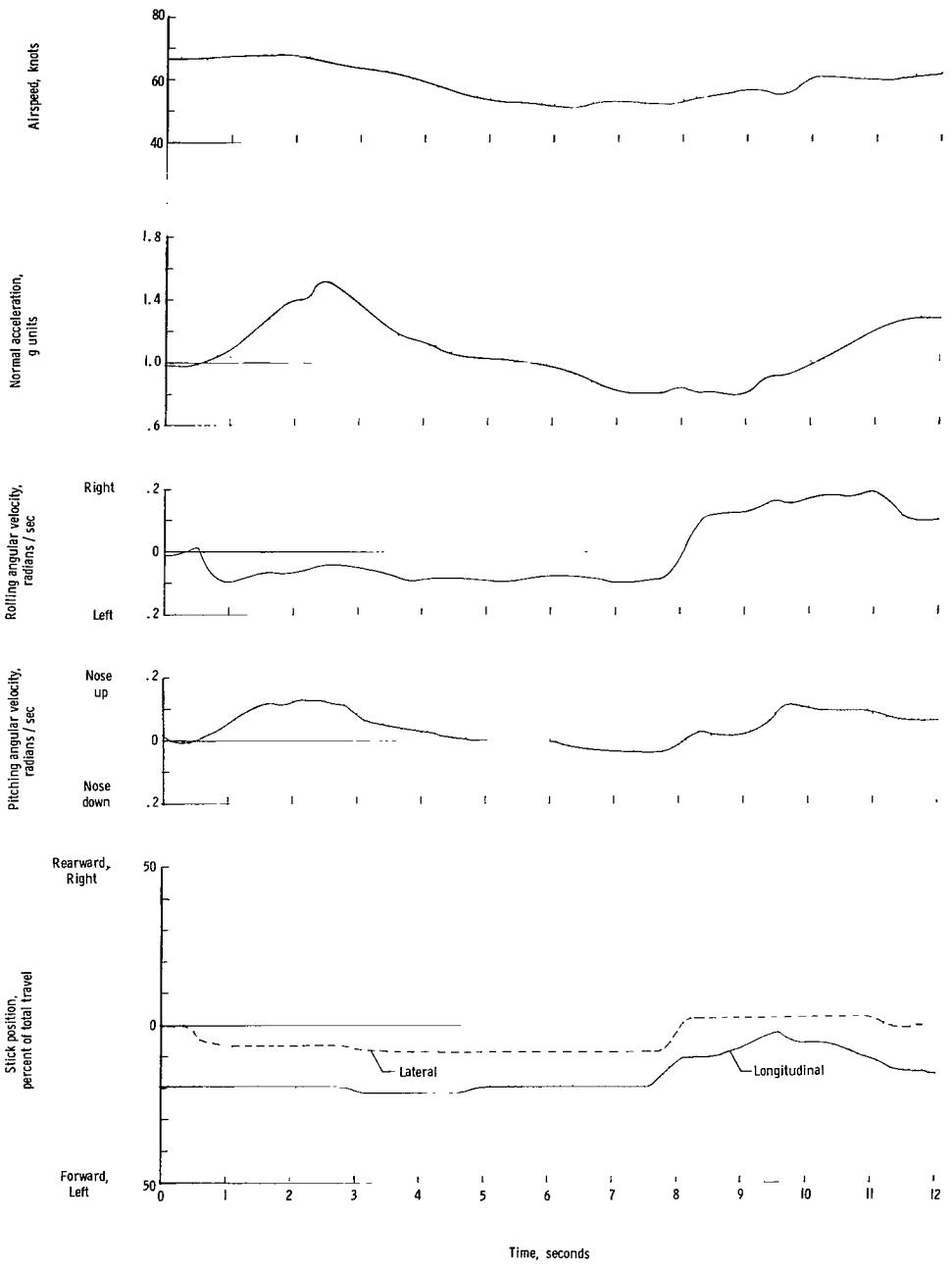

(b) Lateral step input.

Figure 11.- Concluded.

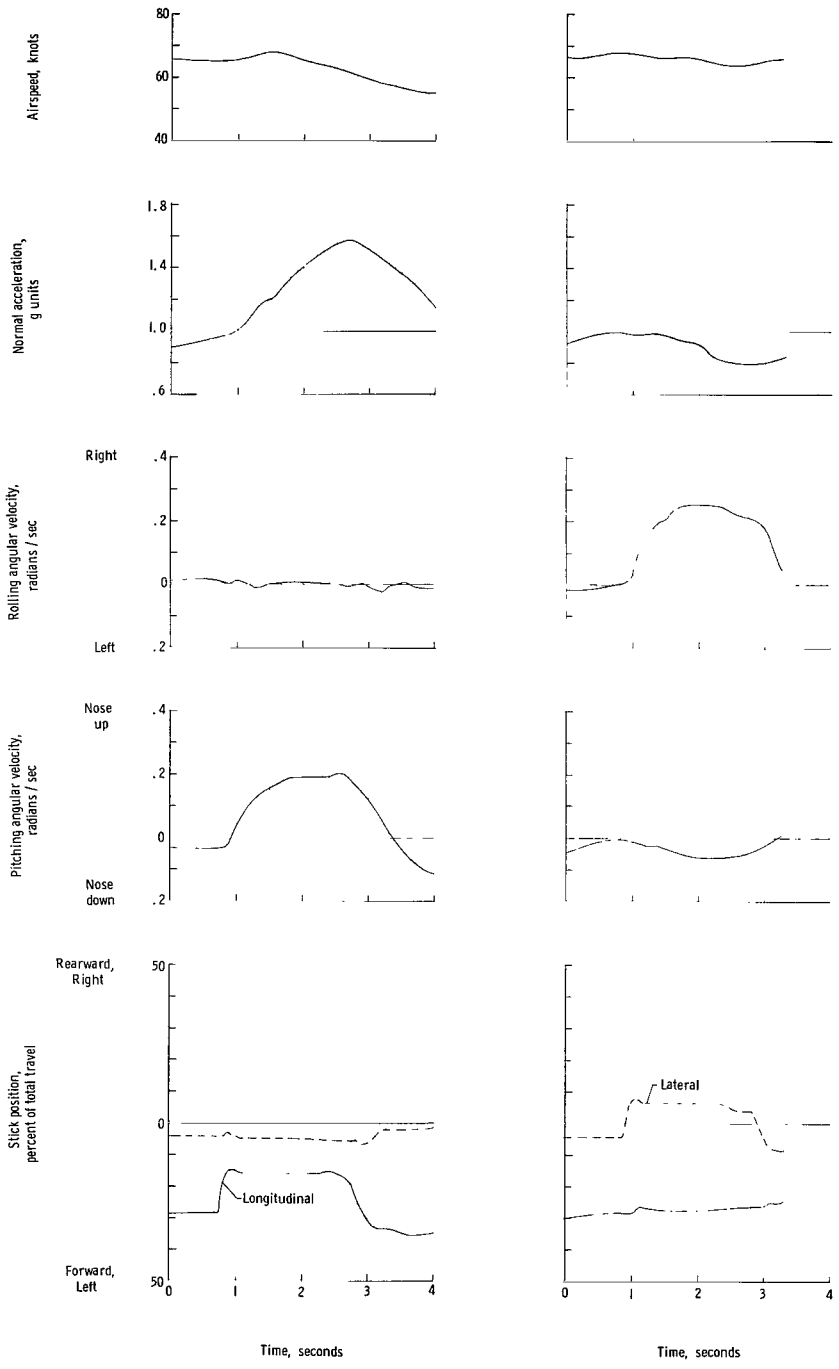

(a) Longitudinal step input.

(b) Lateral step input.

Figure 12.- Time histories of normal acceleration and angular velocities resulting from step control input in forward flight. Teetering rotor.

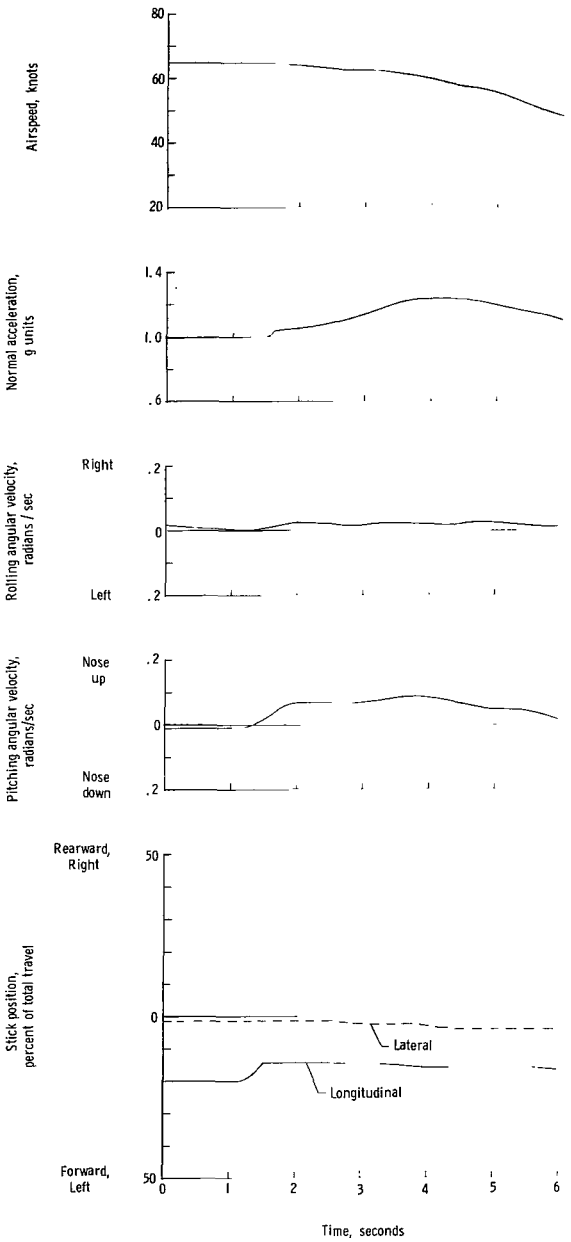

Figure 13.- Time histories of normal acceleration and angular velocities resulting from longitudinal step control input in forward flight. Hingeless rotor helicopter with standard mount installation.

The cross-coupled pitch response to a roll control input is objectionable to the pilot. The pitch up with a left roll (and pitch down with a right roll) resulted in undesirably large normal-acceleration and flight-path changes if control correction was not applied. As in hovering, the pilots considered that accurate control of the pitch attitude during a rolling maneuver was difficult because of the large magnitude of the coupling. A measure of the discomfort of the roll step maneuver to the pilot is seen in figures 10(b) and 11(b) where, when attempting to measure the response without applying a pitch correction, the pilot tends to correct gently with the longitudinal control for the buildup in normal acceleration and pitch rate (fig. 10(b)) or allows it to build to a magnitude where he feels that the pitch rates must be reduced (fig. 11(b)). The use of a longitudinal stick force bobweight (14 pounds per g (62.3 N per g)) which could be engaged by the pilot if desired, did not appreciably affect the pilot's opinion of the cross-coupled response to roll control inputs.

As was the case for hovering maneuvers previously noted, the coupling of roll with pitching velocity in forward flight was considered by the pilots to be of negligible magnitude.

Maneuver Stability

The data obtained show that the hingeless rotor helicopter had positive maneuver stability throughout the speed range. (For example, see figs. 10, 11, and 13.) The requirements of reference 6 specify that

acceptable maneuver stability shall be demonstrated by a normal acceleration time history that is concave downward within 2 seconds after a rearward displacement of the longitudinal control stick. The requirement is met for the stiff mount installation (fig. 10) and nearly met for the standard mount installation (figs. 11 and 13) with the test aircraft. All pilots considered that the maneuver stability obtained with the stiff pylon installation was adequate throughout the speed range. Only one pilot, during his limited evaluation, considered the soft pylon installation to provide unacceptable maneuver stability. The single adverse comment may be attributed to the fact that slightly over 2 seconds were required for the normal acceleration to be concave downward during his test maneuvers at the highest airspeeds, as is shown in figure 13. The main significance of these results is that positive maneuver stability can be obtained with a hingeless rotor without the addition of stability devices, although the degree is affected by the pylon stiffness.

In forward flight, at airspeeds up to the maximum obtainable with the aircraft in level flight, the damping of moderate gust disturbances was considered good by the pilots. The response of the aircraft to longitudinal and lateral control pulses at approximately 65 knots is illustrated in figure 14 for the stiff pylon configuration. No large amplitude oscillations occur, although the short period oscillation that is evident appears

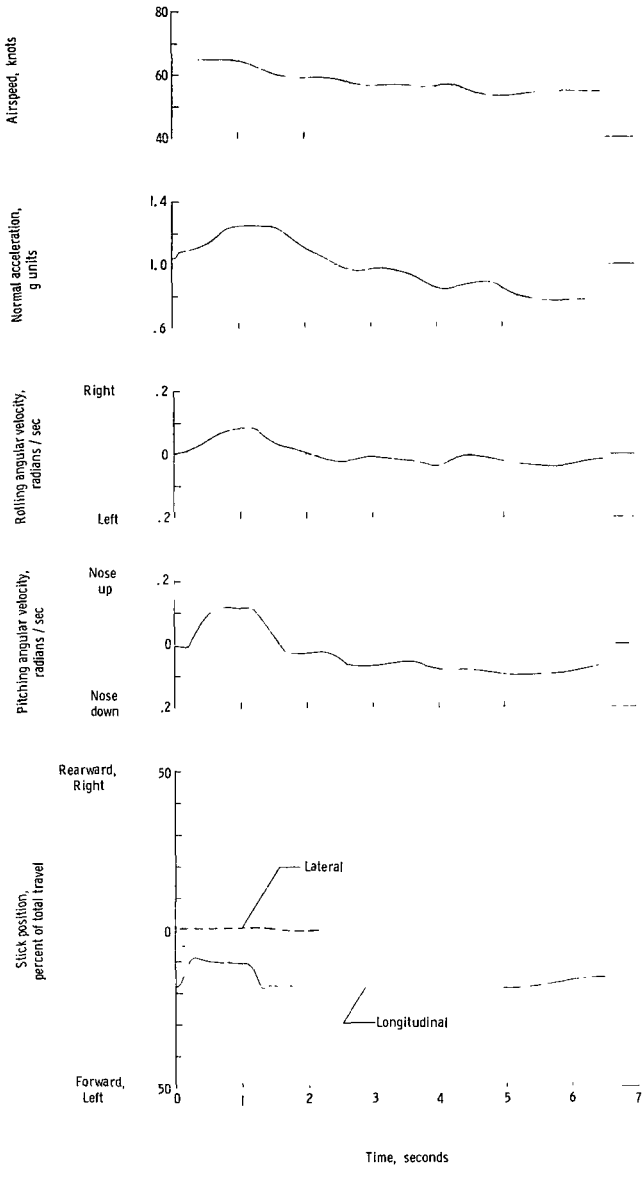

(a) Longitudinal pulse input.

Figure 14.- Time histories of normal acceleration and angular velocities resulting from pulse control input during forward flight. Hingeless rotor helicopter with stiff mount installation.

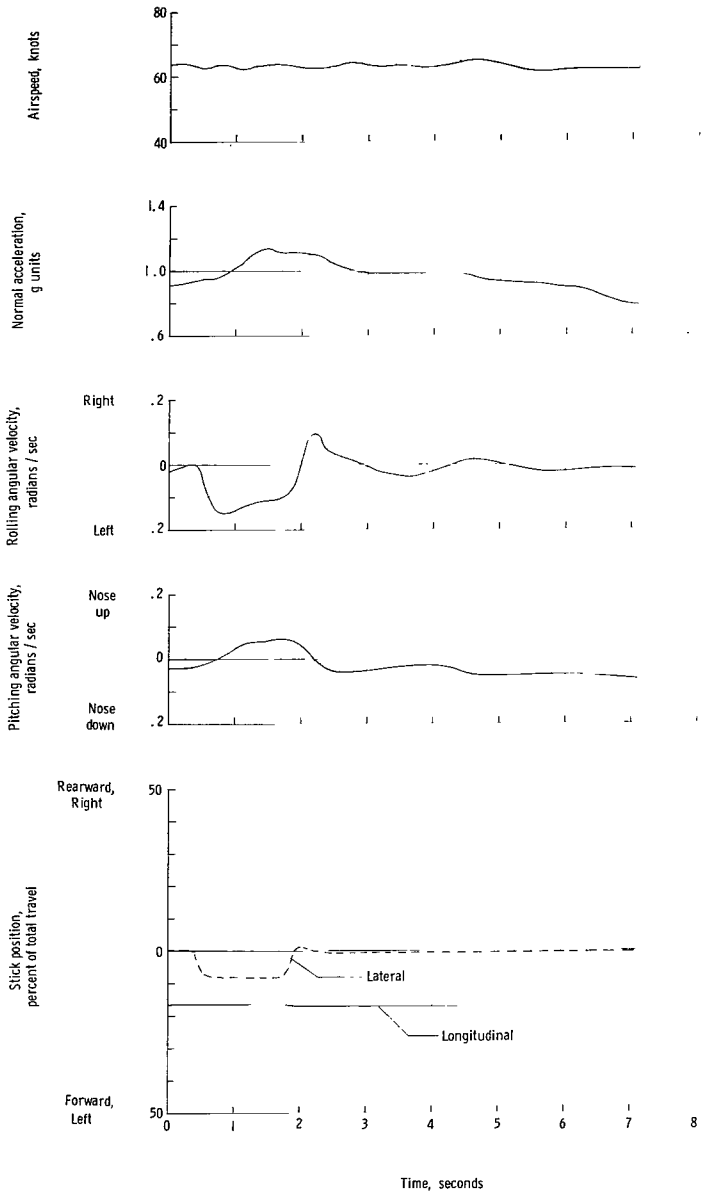

(b) Lateral pulse input.

Figure 14.- Concluded.

to be only moderately damped. The slight cross-coupling between the pitch and roll oscillations does not appear to be a problem to the pilot.

Speed Stability

The longitudinal and lateral stick position with airspeed are presented in figure 15 for several values of aircraft engine power, each with constant collective pitch and rotor speed. The figure shows that the aircraft possessed positive speed stability above approximately 20 knots (i.e., increasing trim airspeed requires a more forward stick position at constant power). The pilots termed this degree of speed stability as adequate. The slight lateral displacement of the stick for trim through the speed range was not apparent to the pilot.

The hingeless rotor helicopter still requires substantially the same cyclic pitch variation with airspeed, at trim conditions, as the articulated rotor helicopter. The variation of blade cyclic pitch and collective pitch for the hingeless rotor helicopter is presented in figure 16 as derived from the trim stick positions using equations (1) and (2).

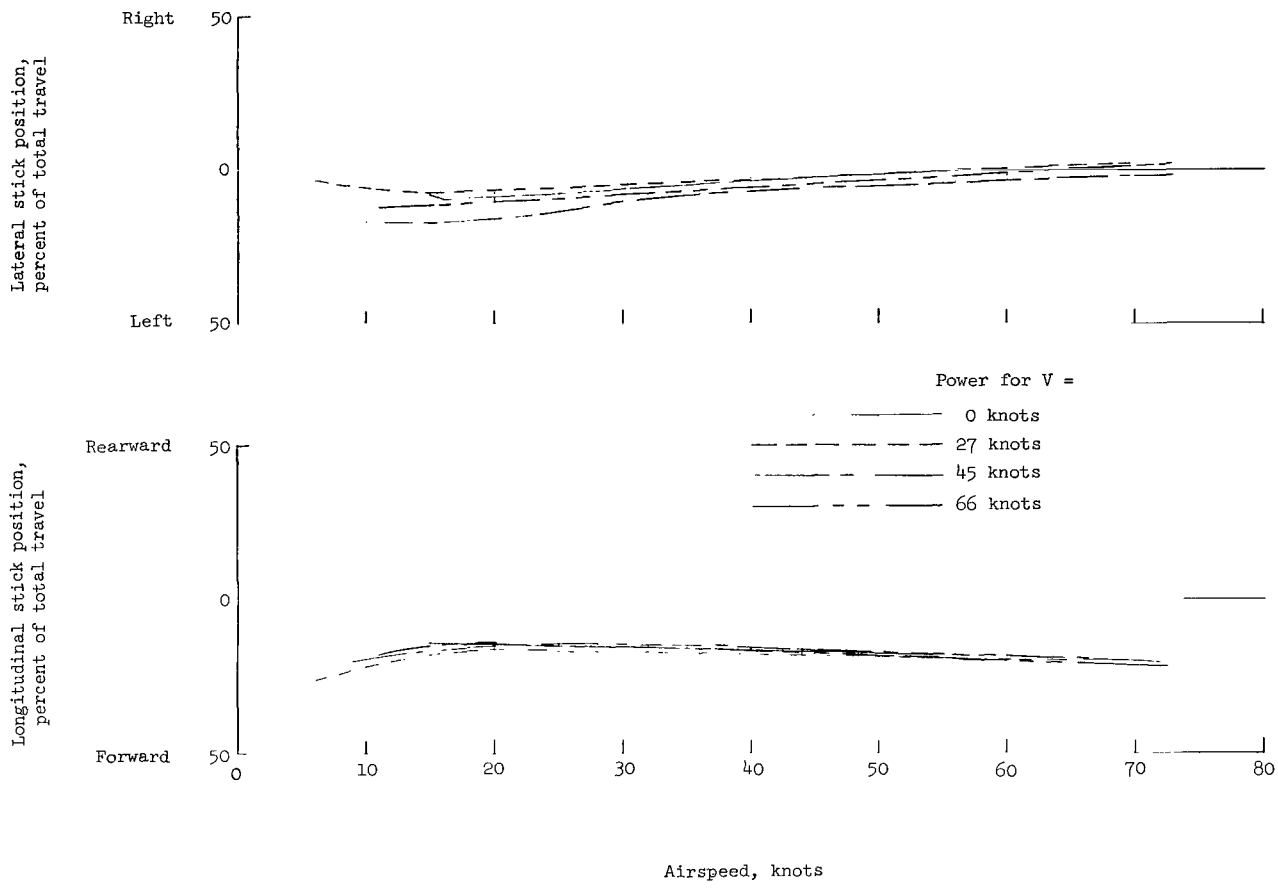

Figure 15.- Variation of longitudinal and lateral stick position with airspeed for four values of constant power. Hingeless rotor helicopter.

General Comments

The "tight" control response available with the hingeless rotor helicopter was generally recognized by pilots as resulting in an improvement in overall handling qualities even though the pitch-roll cross-coupling was termed objectionable by the pilots. It should be noted, however, that methods are available to remove this objectionable problem area; for example, a device to sense the damping coupling and cancel out its effects, as suggested in reference 4. The effect of variations in blade Lock number on the control response characteristics of a hingeless rotor helicopter is discussed in appendix C.

An additional result of this investigation is qualitative confirmation and extension of the results of reference 5 regarding the effects of gyroscopic cross-coupling.

One potential handling qualities problem area that needs further definition is the effect of the structural stiffness of the rotor blades, the control system, the hub, and the rotor pylon and its mounting. The significant differences in both maneuver stability and

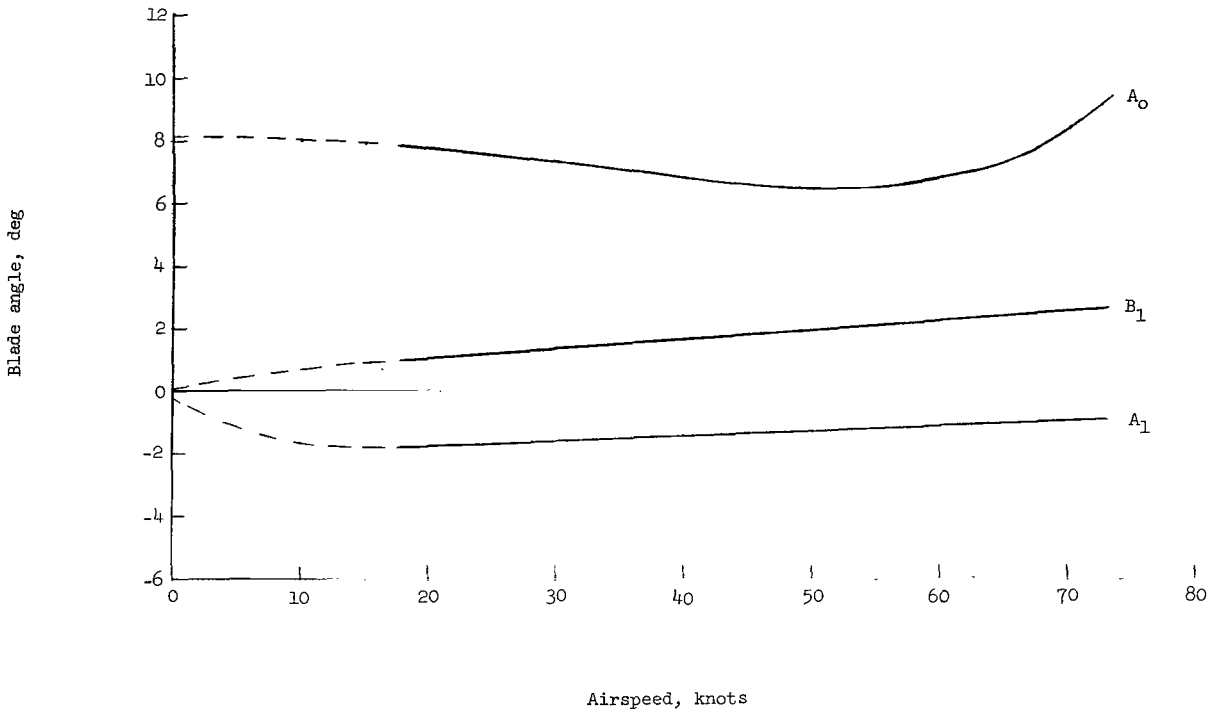

Figure 16.- Variation of blade cyclic pitch and collective pitch with airspeed. Hingeless rotor helicopter. A_0 at 0.75 R.

oscillatory characteristics due to changes in the pylon stiffness indicate that cautious design efforts are required in this area to obtain good handling qualities.

During the flight investigation, the hingeless rotor helicopter was maneuvered throughout the available speed range including vertical autorotation, autorotation at airspeeds up to 70 knots, partial power descents in the vortex ring state, maximum power climb through the speed range, and steep turns in level flight and autorotation. No handling qualtities problems associated with the hingeless rotor configuration were apparent other than those previously described.

CONCLUSIONS

The results of an exploratory handling qualities investigation of a rudimentary hingeless rotor helicopter indicate the following conclusions:

1. The overall hovering control characteristics (control sensitivity and angular-velocity damping) were considered good. Pitch control was positive and precise. The overshoot tendency of the roll response was considered objectionable to the pilots.

2. The most objectionable characteristic of this simple hingeless rotor helicopter was the pitching angular velocities produced by roll control inputs. Analysis indicates that it is the high coupled pitching acceleration that was bothersome to the pilots during hovering maneuvers, with the attendant normal acceleration and flight-path changes becoming bothersome to the pilots in forward flight.

3. The test aircraft, without stabilization devices or a horizontal tail, had positive maneuver stability up to the maximum speed obtainable.

4. Damping of moderate gust disturbances throughout the speed range was considered good by the pilots.

Langley Research Center,
National Aeronautics and Space Administration,
Langley Station, Hampton, Va., January 26, 1966.

APPENDIX A

ANGULAR-VELOCITY RESPONSE OF A HINGELESS ROTOR HELICOPTER

By Robert J. Huston and William J. Snyder

For a simultaneous two-axis displacement-and-hold type of control input, the equations of motion about the lateral and longitudinal axes, respectively, for an aircraft with direct control coupling and gyroscopic cross-coupling are:

$$\left.\begin{aligned}\dot{p} + \frac{M_p}{I_X} p + \frac{H}{I_X} q &= \delta_x\left(\frac{M_{x\delta_x}}{I_X}\right) + \delta_y\left(\frac{M_{x\delta_y}}{I_X}\right)\\ \dot{q} + \frac{M_q}{I_Y} q - \frac{H}{I_Y} p &= \delta_x\left(\frac{M_{y\delta_x}}{I_Y}\right) + \delta_y\left(\frac{M_{y\delta_y}}{I_Y}\right)\end{aligned}\right\} \tag{A1}$$

The solutions to equations (A1) are given by the following two equations for the initial conditions of $p = q = 0$ when

$$\left(\frac{M_p}{I_X} - \frac{M_q}{I_Y}\right)^2 - \frac{4H^2}{I_X I_Y} \geqq 0$$

$$p = \left[\delta_x\left(\frac{M_{x\delta_x} M_q - M_{y\delta_x} H}{H^2 + M_p M_q}\right) + \delta_y\left(\frac{M_{x\delta_y} M_q - M_{y\delta_y} H}{H^2 + M_p M_q}\right)\right]\left\{1 - \left[\frac{B}{\sqrt{C}} \sinh\left(\frac{t}{2}\sqrt{C}\right) + \cosh\left(\frac{t}{2}\sqrt{C}\right)\right]\exp\left(-\frac{t}{2} B\right)\right\} + \left[\delta_x\left(\frac{M_{x\delta_x}}{I_X}\right) + \delta_y\left(\frac{M_{x\delta_y}}{I_X}\right)\right]\left[\frac{2}{\sqrt{C}} \sinh\left(\frac{t}{2}\sqrt{C}\right)\right]\exp\left(-\frac{t}{2} B\right) \tag{A2a}$$

$$q = \left[\delta_x\left(\frac{M_{x\delta_x} H + M_{y\delta_x} M_p}{H^2 + M_p M_q}\right) + \delta_y\left(\frac{M_{x\delta_y} H + M_{y\delta_y} M_p}{H^2 + M_p M_q}\right)\right]\left\{1 - \left[\frac{B}{\sqrt{C}} \sinh\left(\frac{t}{2}\sqrt{C}\right) + \cosh\left(\frac{t}{2}\sqrt{C}\right)\right]\exp\left(-\frac{t}{2} B\right)\right\} + \left[\delta_x\left(\frac{M_{y\delta_x}}{I_Y}\right) + \delta_y\left(\frac{M_{y\delta_y}}{I_Y}\right)\right]\left[\frac{2}{\sqrt{C}} \sinh\left(\frac{t}{2}\sqrt{C}\right)\right]\exp\left(-\frac{t}{2} B\right) \tag{A2b}$$

where

$$B = \frac{M_p}{I_X} + \frac{M_q}{I_Y} \qquad C = \left(\frac{M_p}{I_X} - \frac{M_q}{I_Y}\right)^2 - \frac{4H^2}{I_X I_Y}$$

when $\left(\frac{M_p}{I_X} - \frac{M_q}{I_Y}\right)^2 - \frac{4H^2}{I_X I_Y} < 0$, the solutions to equations (A1) are given by

$$p = \left[\delta_x\left(\frac{M_{x\delta_x} M_q - M_{y\delta_x} H}{H^2 + M_p M_q}\right) + \delta_y\left(\frac{M_{x\delta_y} M_q - M_{y\delta_y} H}{H^2 + M_p M_q}\right)\right]\left\{1 + 2A\left[\sin\left(\frac{t}{2}\sqrt{-C}\right.\right.\right.$$

$$\left.\left.\left. - \tan^{-1}\frac{\sqrt{-C}}{-B}\right)\right]\exp\left(-\frac{t}{2}B\right)\right\} + \left[\delta_x\left(\frac{M_{x\delta_x}}{I_X}\right) + \delta_y\left(\frac{M_{x\delta_y}}{I_X}\right)\right]\left[\frac{2}{\sqrt{-C}}\sin\left(\frac{t}{2}\sqrt{-C}\right)\right]\exp\left(-\frac{t}{2}B\right) \quad \text{(A3a)}$$

$$q = \left[\delta_x\left(\frac{M_{x\delta_x} H + M_{y\delta_x} M_p}{H^2 + M_p M_q}\right) + \delta_y\left(\frac{M_{x\delta_y} H + M_{y\delta_y} M_p}{H^2 + M_p M_q}\right)\right]\left\{1 + 2A\left[\sin\left(\frac{t}{2}\sqrt{-C}\right.\right.\right.$$

$$\left.\left.\left. - \tan^{-1}\frac{\sqrt{-C}}{-B}\right)\right]\exp\left(-\frac{t}{2}B\right)\right\} + \left[\delta_x\left(\frac{M_{y\delta_x}}{I_Y}\right) + \delta_y\left(\frac{M_{y\delta_y}}{I_Y}\right)\right]\left[\frac{2}{\sqrt{-C}}\sin\left(\frac{t}{2}\sqrt{-C}\right)\right]\exp\left(-\frac{t}{2}B\right) \quad \text{(A3b)}$$

where

$$A = \sqrt{\frac{C - B^2}{4C}}$$

At $t = \infty$, equations (A2) and (A3) simplify to

$$p_\infty = \delta_x\left(\frac{M_{x\delta_x} M_q - M_{y\delta_x} H}{H^2 + M_p M_q}\right) + \delta_y\left(\frac{M_{x\delta_y} M_q - M_{y\delta_y} H}{H^2 + M_p M_q}\right) \quad \text{(A4a)}$$

$$q_\infty = \delta_x\left(\frac{M_{x\delta_x} H + M_{y\delta_x} M_p}{H^2 + M_p M_q}\right) + \delta_y\left(\frac{M_{x\delta_y} H + M_{y\delta_y} M_p}{H^2 + M_p M_q}\right) \quad \text{(A4b)}$$

The longitudinal stick displacement required to trim the final pitching velocity to zero during a steady-state rolling maneuver, determined by setting equation (A4b) equal to zero, is

$$\delta_{y,trim} = -\delta_x\left(\frac{M_{x_{\delta_x}} H + M_{y_{\delta_x}} M_p}{M_{x_{\delta_y}} H + M_{y_{\delta_y}} M_p}\right) \tag{A5}$$

and in a similar manner, the lateral stick displacement required to trim the final rolling velocity to zero during a steady-state pitching maneuver is

$$\delta_{x,trim} = -\delta_y\left(\frac{M_{x_{\delta_y}} M_q - M_{y_{\delta_y}} H}{M_{x_{\delta_x}} M_q - M_{y_{\delta_x}} H}\right) \tag{A6}$$

For the case of no direct control coupling $\left(M_{y_{\delta_x}} = M_{x_{\delta_y}} = 0\right)$ and for a single axis control input, the ratio of final angular velocities obtained from equation (A4) is

for $\delta_y = 0$

$$\frac{q_\infty}{p_\infty} = \frac{H}{M_q} \tag{A7}$$

and for $\delta_x = 0$

$$\frac{p_\infty}{q_\infty} = -\frac{H}{M_p} \tag{A8}$$

APPENDIX B

COMPUTED CHARACTERISTICS OF THE HINGELESS ROTOR OH-13 HELICOPTER

For the hingeless rotor OH-13 helicopter, the cyclic pitch input due to longitudinal and lateral stick motion, with control retardation, can be written as

$$A_1 = \left(\frac{\Delta\theta}{\Delta\delta_x}\right)_{max} (\cos\epsilon)\delta_x + \left(\frac{\Delta\theta}{\Delta\delta_y}\right)_{max} (\sin\epsilon)\delta_y \tag{B1a}$$

$$B_1 = \left(\frac{\Delta\theta}{\Delta\delta_x}\right)_{max} (\sin\epsilon)\delta_x - \left(\frac{\Delta\theta}{\Delta\delta_y}\right)_{max} (\cos\epsilon)\delta_y \tag{B1b}$$

The ingredients for the equations of motion of appendix A (eqs. A1) may be written as

$$M_{x_{\delta_x}} = \left\{\left[\Delta\left(\frac{M_B}{I_V\Omega^2}\right)_{B_1}\right]\sin\epsilon + \left[\Delta\left(\frac{M_B}{I_V\Omega^2}\right)_{A_1}\right]\cos\epsilon\right\}\left(\frac{\Delta\theta}{\Delta\delta_x}\right)_{max} I_V\Omega^2 \tag{B2}$$

$$M_{x_{\delta_y}} = \left\{\left[\Delta\left(\frac{M_B}{I_V\Omega^2}\right)_{B_1}\right](-\cos\epsilon) + \left[\Delta\left(\frac{M_B}{I_V\Omega^2}\right)_{A_1}\right]\sin\epsilon\right\}\left(\frac{\Delta\theta}{\Delta\delta_y}\right)_{max} I_V\Omega^2 \tag{B3}$$

$$M_{y_{\delta_x}} = \left\{\left[\Delta\left(\frac{M_A}{I_V\Omega^2}\right)_{B_1}\right]\sin\epsilon + \left[\Delta\left(\frac{M_A}{I_V\Omega^2}\right)_{A_1}\right]\cos\epsilon\right\}\left(\frac{\Delta\theta}{\Delta\delta_x}\right)_{max} I_V\Omega^2 \tag{B4}$$

$$M_{y_{\delta_y}} = \left\{\left[\Delta\left(\frac{M_A}{I_V\Omega^2}\right)_{B_1}\right](-\cos\epsilon) + \left[\Delta\left(\frac{M_A}{I_V\Omega^2}\right)_{A_1}\right]\sin\epsilon\right\}\left(\frac{\Delta\theta}{\Delta\delta_y}\right)_{max} I_V\Omega^2 \tag{B5}$$

$$M_p = -\left[\Delta\left(\frac{M_B}{I_V\Omega}\right)_p\right] I_V\Omega \tag{B6}$$

$$M_q = -\left[\Delta\left(\frac{M_A}{I_V\Omega}\right)_q\right] I_V\Omega \tag{B7}$$

$$H = -\left[\Delta\left(\frac{M_B}{I_V\Omega}\right)_q\right] I_V\Omega = \left[\Delta\left(\frac{M_A}{I_V\Omega}\right)_p\right] I_V\Omega \tag{B8}$$

APPENDIX B

The value of the hub moment increments in equations (B2) to (B8) is calculated by using the procedures of references 3 and 4 for $\gamma = 3.85$ and $\omega_{1NR}/\Omega = 0.185$ and is presented in figures 17 and 18. The direct hub moment increments are increased to account for thrust vector tilt due to cyclic pitch and thrust vector lag due to pitching and rolling velocities. For these calculations, the thrust vector tilt and lag were considered to be 100 percent effective; that is, there was no reduction in tip-path-plane tilt or following rate due to rotor flapping stiffness. The complete moment increments, including the effect of thrust vector lag and tilt, are known from the following equations:

$$\Delta\left(\frac{M_B}{I_V\Omega^2}\right)_{B_1} = \Delta\left(\frac{M_{H,B}}{I_V\Omega^2}\right)_{B_1} \tag{B9}$$

$$\Delta\left(\frac{M_B}{I_V\Omega^2}\right)_{A_1} = \Delta\left(\frac{M_{H,B}}{I_V\Omega^2}\right)_{A_1} + \frac{Th}{I_V\Omega^2} \tag{B10}$$

$$\Delta\left(\frac{M_A}{I_V\Omega^2}\right)_{B_1} = \Delta\left(\frac{M_{H,A}}{I_V\Omega^2}\right)_{B_1} - \frac{Th}{I_V\Omega^2} \tag{B11}$$

$$\Delta\left(\frac{M_A}{I_V\Omega^2}\right)_{A_1} = \Delta\left(\frac{M_{H,A}}{I_V\Omega^2}\right)_{A_1} \tag{B12}$$

$$\Delta\left(\frac{M_B}{I_V\Omega}\right)_p = \Delta\left(\frac{M_{H,B}}{I_V\Omega}\right)_p + \frac{Th}{I_V\Omega}\left(\frac{\Delta b'}{p}\right) \tag{B13}$$

when

$$\frac{\Delta b'}{p} = -\frac{27}{\gamma\Omega}\left(1.0 - 0.29\,\frac{A_o}{C_T/\sigma}\right) \tag{B14}$$

$$\Delta\left(\frac{M_A}{I_V\Omega}\right)_q = \Delta\left(\frac{M_{H,A}}{I_V\Omega}\right)_q + \frac{Th}{I_V\Omega}\left(\frac{\Delta a'}{q}\right) \tag{B15}$$

when

$$\frac{\Delta a'}{q} = -\frac{27}{\gamma\Omega}\left(1.0 - 0.29\,\frac{A_o}{C_T/\sigma}\right) \tag{B16}$$

$$\Delta\left(\frac{M_B}{I_V\Omega}\right)_q = \Delta\left(\frac{M_{H,B}}{I_V\Omega}\right)_q \tag{B17}$$

$$\Delta\left(\frac{M_A}{I_V\Omega}\right)_p = \Delta\left(\frac{M_{H,A}}{I_V\Omega}\right)_p \tag{B18}$$

The computed hub moment increments with respect to cyclic pitch and pitching and rolling velocities are presented in the following table:

Contribution due to direct hub moment (figs. 17 and 18)	Ingredients for equations (B2) to (B8)
$\Delta\left(\frac{M_{H,B}}{I_V\Omega^2}\right)_{B_1} = 0.155$	$\Delta\left(\frac{M_B}{I_V\Omega^2}\right)_{B_1} = 0.155$
$\Delta\left(\frac{M_{H,B}}{I_V\Omega^2}\right)_{A_1} = 0.210$	$\Delta\left(\frac{M_B}{I_V\Omega^2}\right)_{A_1} = 0.250$
$\Delta\left(\frac{M_{H,A}}{I_V\Omega^2}\right)_{B_1} = -0.210$	$\Delta\left(\frac{M_A}{I_V\Omega^2}\right)_{B_1} = -0.250$
$\Delta\left(\frac{M_{H,A}}{I_V\Omega^2}\right)_{A_1} = 0.155$	$\Delta\left(\frac{M_A}{I_V\Omega^2}\right)_{A_1} = 0.155$
$\Delta\left(\frac{M_{H,B}}{I_V\Omega}\right)_p = -1.60$	$\Delta\left(\frac{M_B}{I_V\Omega}\right)_p = -1.73$
$\Delta\left(\frac{M_{H,A}}{I_V\Omega}\right)_q = -1.60$	$\Delta\left(\frac{M_A}{I_V\Omega}\right)_q = -1.73$
$\Delta\left(\frac{M_{H,B}}{I_V\Omega}\right)_q = 0.80$	$\Delta\left(\frac{M_B}{I_V\Omega}\right)_q = 0.80$
$\Delta\left(\frac{M_{H,A}}{I_V\Omega}\right)_p = -0.80$	$\Delta\left(\frac{M_A}{I_V\Omega}\right)_p = -0.80$

APPENDIX C

EFFECT OF BLADE MASS CONSTANT (LOCK NUMBER) ON THE CONTROL RESPONSE CHARACTERISTICS OF A HINGELESS ROTOR HELICOPTER

It became apparent during the analysis for this paper that the design choice for a value of the blade Lock number is a factor which may significantly affect the handling qualities of a hingeless rotor helicopter. The blade Lock number is the ratio of blade air forces to blade mass forces $\left(\frac{\rho acR^4}{I_V}\right)$. An increase in blade weight, other factors being held constant, results in a reduction in blade Lock number.

The effect of combinations of blade Lock number and blade stiffness on the nondimensional rotor hub control moment per unit of cyclic pitch and damping moment per unit of aircraft angular velocity is presented in figures 17 and 18. These two figures are reproduced from reference 3 and are the source of the ingredients for equations (B2) to (B8). Current cantilever blade designs have a nonrotating flapwise frequency ratio ω_{1NR}/Ω on the order of 0.2 and there is little variation between designs. The range of Lock numbers at standard air density, however, varies from values below 4 to more than 8.

The data of figure 17 can be used to show that there is little effect of a change in blade Lock number on the total control moment $\sqrt{\left[\Delta\left(\frac{M_{H,B}}{I_V\Omega^2}\right)_{A_1}\right]^2 + \left[\Delta\left(\frac{M_{H,A}}{I_V\Omega^2}\right)_{A_1}\right]^2}$ available for the normal values of flapwise natural frequency. However, a reduction of blade Lock number from a value of 8 to 4, for example, results in a substantial increase in the coupling moment. This increased coupling would require a corresponding increase in the required control retardation angle previously discussed. It should be noted that a change in blade Lock number thereby results in a different level of the ratio of damping to critical damping, where the damping referred to is the damping of the first flapwise mode of the blade.

The effect of a reduction in blade Lock number on the aircraft angular velocity damping is shown in figure 18. The direct damping moment is substantially increased with a reduction in blade Lock number from 8 to 4, for example. An adverse effect, however, is the increase in the damping moment term that produces a gyroscopic control coupling from essentially zero to approximately half of the direct damping moment.

APPENDIX C

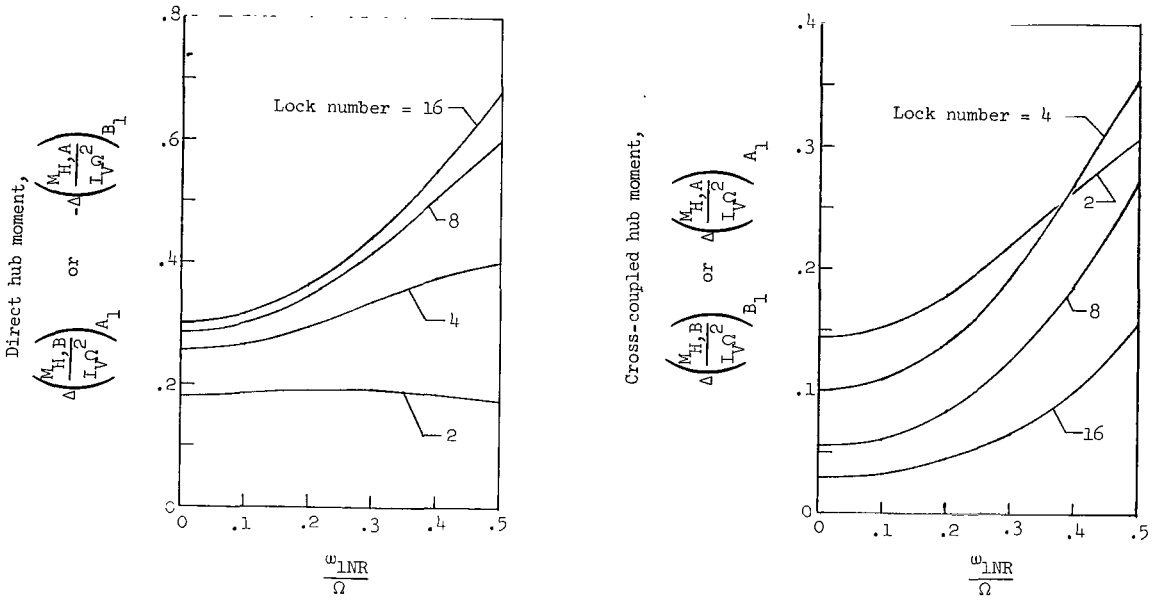

Figure 17.- Effect of blade Lock number and blade stiffness on rotor hub control moments. Three blade rotor.

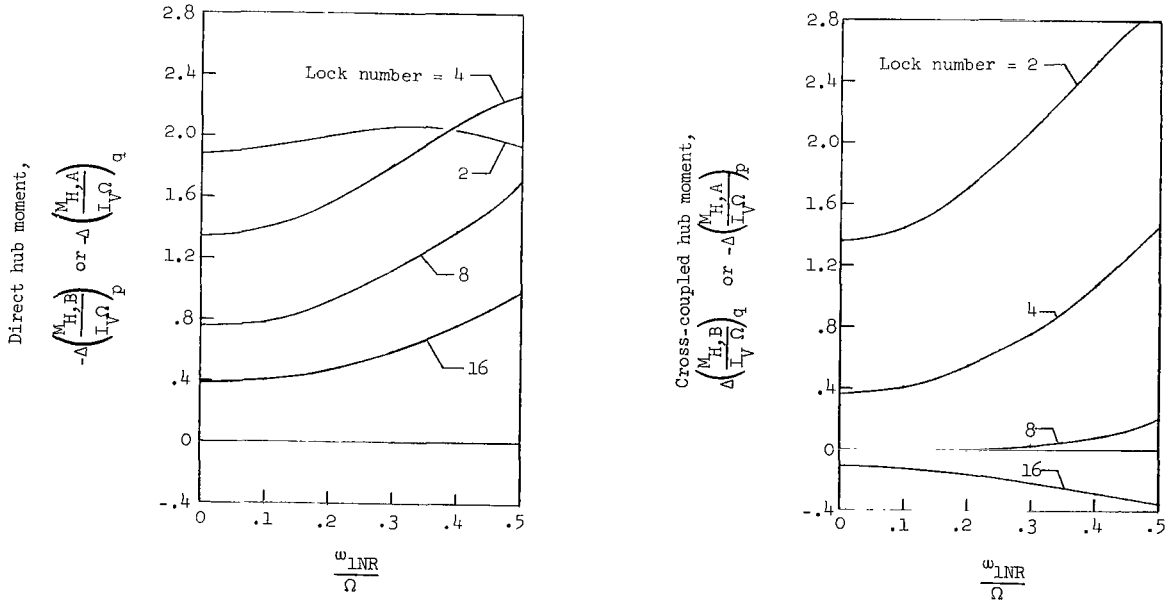

Figure 18.- Effect of blade Lock number and blade stiffness on rotor hub damping moments. Three blade rotor.

APPENDIX C

The rudimentary nature of the hingeless rotor helicopter used in this flight investigation resulted in a particularly unfortunate choice of blade Lock numbers (γ = 3.85). The dynamics associated with a Lock number this small can be expected to present a much more serious gyroscopic coupling problem to a pilot than a rotor with a blade Lock number of 8.0, for example.

An even more important point for consideration in future designs is the effect of density altitude on control characteristics and control response. The blade Lock number is directly proportional to the mass density of the air. Therefore, large variations in operating density altitude, which may be expected of turbine powered helicopters under operational use, can result both in severe direct cross-coupling and in severe gyroscopic coupling at altitudes even if these effects are not present at standard air density. It appears that in order to eliminate completely all coupling effects accompanying changes in density altitude, special provision would have to be made to vary control retardation with density altitude and to provide some type of feedback device which is sensitive to aircraft angular velocity. A design giving zero coupling at some intermediate altitude may minimize the effects at both extremes of altitude sufficiently for many applications and minimize the requirements for special devices in other cases.

The equations of motion presented in appendix A may be used to study the effects of density altitude in order to minimize the handling qualities problems presented by the cross-coupled response of a hingeless rotor helicopter.

REFERENCES

1. Cresap, W. L.: Rigid Rotor Development and Flight Tests. Paper No. 62-17, Inst. Aerospace Sci., Jan. 1962.

2. Huston, Robert J.; and Tapscott, Robert J.: Results of Some Wind Tunnel and Flight Studies With Helicopters at NASA. Vertical Take-Off and Landing (VTOL) Aircraft. Ann. N.Y. Acad. Sci., vol. 106, art. 1, Mar. 1963, pp. 57-69.

3. Ward, John F.; and Huston, Robert J.: A Summary of Hingeless-Rotor Research at NASA – Langley. Proc. Twentieth Ann. Nat. Forum, Am. Helicopter Soc., Inc., May 1964, pp. 76-83.

4. Young, Maurice I.: A Simplified Theory of Hingeless Rotors With Application to Tandem Helicopters. Proc. Eighteenth Ann. Nat. Forum, Am. Helicopter Soc., Inc., May 1962, pp. 38-45.

5. Garren, John F., Jr.: Effects of Gyroscopic Cross Coupling Between Pitch and Roll on the Handling Qualities of VTOL Aircraft. NASA TN D-812, 1961.

6. Anon.: Helicopter Flying and Ground Handling Qualities; General Requirements for. Mil. Specification MIL-H-8501A, Sept. 7, 1961.

"The aeronautical and space activities of the United States shall be conducted so as to contribute . . . to the expansion of human knowledge of phenomena in the atmosphere and space. The Administration shall provide for the widest practicable and appropriate dissemination of information concerning its activities and the results thereof."

—NATIONAL AERONAUTICS AND SPACE ACT OF 1958

NASA SCIENTIFIC AND TECHNICAL PUBLICATIONS

TECHNICAL REPORTS: Scientific and technical information considered important, complete, and a lasting contribution to existing knowledge.

TECHNICAL NOTES: Information less broad in scope but nevertheless of importance as a contribution to existing knowledge.

TECHNICAL MEMORANDUMS: Information receiving limited distribution because of preliminary data, security classification, or other reasons.

CONTRACTOR REPORTS: Technical information generated in connection with a NASA contract or grant and released under NASA auspices.

TECHNICAL TRANSLATIONS: Information published in a foreign language considered to merit NASA distribution in English.

TECHNICAL REPRINTS: Information derived from NASA activities and initially published in the form of journal articles.

SPECIAL PUBLICATIONS: Information derived from or of value to NASA activities but not necessarily reporting the results of individual NASA-programmed scientific efforts. Publications include conference proceedings, monographs, data compilations, handbooks, sourcebooks, and special bibliographies.

Details on the availability of these publications may be obtained from:

SCIENTIFIC AND TECHNICAL INFORMATION DIVISION

NATIONAL AERONAUTICS AND SPACE ADMINISTRATION

Washington, D.C. 20546